

Effects of ion bombardment on a two-dimensional target: Atomistic simulations of graphene irradiation

O. Lehtinen,¹ J. Kotakoski,¹ A. V. Krasheninnikov,^{1,2} A. Tolvanen,¹ K. Nordlund,¹ and J. Keinonen¹

¹*Materials Physics Division, University of Helsinki, P.O. Box 43, FI-00014 Helsinki, Finland*

²*Department of Applied Physics, Aalto University, P.O. Box 1100, FI-00076 Aalto, Finland*

(Received 2 March 2010; published 1 April 2010)

Using atomistic computer simulations based on analytical potential and density-functional theory models, we study effects of ion irradiation on graphene. We identify the types and concentrations of defects which appear in graphene under impacts of various ions with energies ranging from tens of electron volts to mega-electron volts. For two-dimensional targets, defects beyond single and double vacancies are formed via in-plane recoils. We demonstrate that the conventional approach based on binary-collision approximation and stochastic algorithms developed for bulk solids cannot be applied to graphene and other low-dimensional systems. Finally, taking into account the gas-holding capacity of graphene, we suggest the use of graphene as the ultimate membrane for ion-beam analysis of gases and other volatile systems which cannot be put in the high vacuum required for the operation of ion beams.

DOI: [10.1103/PhysRevB.81.153401](https://doi.org/10.1103/PhysRevB.81.153401)

PACS number(s): 61.80.Az, 61.48.Gh, 61.80.Jh

Graphene, the ultimately thin membrane made from sp^2 -hybridized carbon atoms, has attracted enormous attention since its discovery,¹ mainly due to its unique electronic properties.² In this context, effects of disorder on the electronic structure and on the operation of graphene-based electronic devices have been extensively studied.^{3,4} To assess the role of disorder, ion irradiation^{4–7} has been used to introduce defects in graphene, followed by characterization of the irradiated samples by various techniques.

The correct interpretation of these experiments is not possible without the precise microscopic knowledge of the damage production mechanisms and defects created by the energetic ions in the sample. In bulk materials, after nearly half-century-long intensive research,⁸ the concentration of irradiation-induced defects in the target can be estimated quite accurately within a semiempirical approach based on the binary-collision (BC) approximation, combined with statistical algorithms to calculate how a moving ion transfers its energy to the target atoms.⁹ This approach, implemented in a computer code TRIM, gives reasonable results for bulk targets.¹⁰ However, it may not directly be applicable to low-dimensional systems; the sample is treated as an amorphous matrix with a homogeneous mass density while the explicit account for the atomic structure is very important in assessing the effects of irradiation on nanosystems.¹¹

In this Brief Report, by using molecular dynamics (MD) combined with the analytical potential (AP) and density-functional theory (DFT) methods, we simulate impacts of energetic ions onto suspended graphene sheets and single-walled carbon nanotubes (SWNTs). We demonstrate that the conventional approach developed for bulk solids cannot be applied to graphene and other low-dimensional systems. We identify the types and abundance of defects which appear in graphene under irradiation with various ions having energies ranging from tens of electron volt to mega-electron volt. Finally, taking into account the gas-holding capacity of graphene,^{6,12} we point out the possibility of using graphene as the ultimate membrane for studying irradiation effects in gases, works of art, living cells, and other volatile systems

which cannot be put in high vacuum required for the operation of ion beams.

It is well known that energy loss of relatively heavy and slow ions moving in any solid is dominated by the collisions of the moving ion with the atoms,⁸ which can be reliably modeled using classical MD simulations within the Born-Oppenheimer approximation. Although deposition of energy into electronic degrees of freedom of graphene also occurs under impacts of energetic ions,¹³ this effect should not substantially increase defect production for the ion types and energies considered in this work because graphene is an excellent heat and charge conductor. Following our previous work on ion irradiation of carbon nanotubes,¹⁴ we used a reactive analytical bond order potential to describe carbon-carbon interaction.¹⁵ This approach is computationally efficient enough for collecting significant statistics when simulating impacts of energetic ions onto nanoscale systems while explicitly taking into account their atomic structure. To validate this approach, we also used MD DFT calculations for irradiation simulations as described below. Note that for direct analogy with experiments, we refer to the incoming atom as an “ion” throughout the text. The atom’s charge was not explicitly considered since effects of low charge states are negligible.

The target system in AP MD simulations consisted of 800 carbon atoms and the dissipation of the kinetic energy brought in by an energetic ion was taken into account through the Berendsen thermostat¹⁶ at the borders of the system, see Fig. 1(a). The impact points were randomly selected within the minimum irreducible area in the primitive cell of graphene. We carried out 1500 independent simulations for each ion and energy (a total of 150 000 runs). The interaction between noble gas ions (He, Ne, Ar, Kr, and Xe) and carbon atoms was described by the Ziegler-Biersack-Littmark universal repulsive potential.⁹

We started the analysis of ion bombardment simulations by calculating the average number of sputtered target atoms as a function of ion energy, see Fig. 1(b). Examination of the atomic structure after the impacts revealed that the most pro-

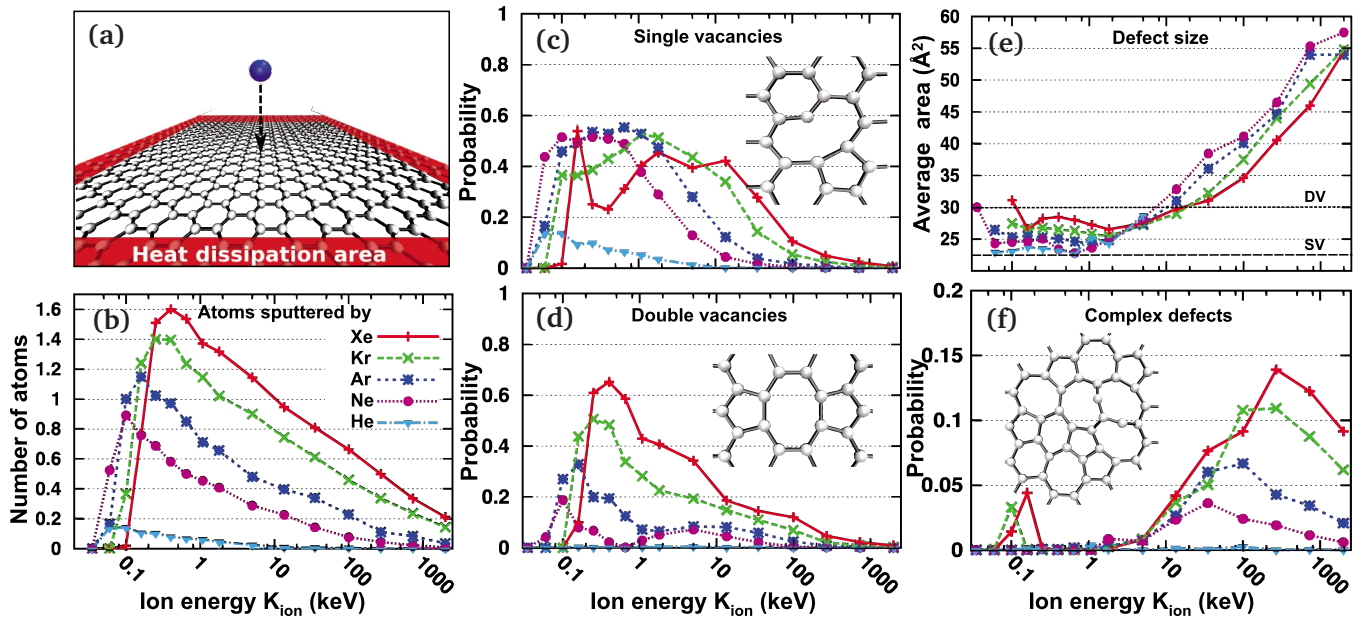


FIG. 1. (Color online) Production of defects in graphene under ion irradiation as revealed by the analytical potential molecular dynamics. (a) Simulation setup. (b) Number of sputtered atoms per ion impact as a function of ion energy. [(c) and (d)] Probability for single and double vacancy formation as a function of ion energy. The insets show the atomic structures of the reconstructed vacancies. (e) Average area covered by a single defect (when formed)—typically still an sp^2 -bonded network of carbon atoms. The areas corresponding to a SV and DV are marked. (f) Probability for creating defects other than SV/DV (except FP/SW, see text), see the inset for an example.

lific defects associated with the sputtered atoms are single¹⁷ and double¹⁸ vacancies (SV and DV, respectively). Besides SV and DV, we observed some triple vacancies, spatially close Frenkel pairs (FP), i.e., adatom-vacancy pairs and Stone-Wales defects¹⁹ but they were rather rare (maximum combined probability less than 9%). The probability for SVs and DVs to appear has an ion-dependent maximum, especially for DVs, as seen in Figs. 1(c) and 1(d). The initial increase with ion energy can easily be understood, as low-energy ions simply cannot displace target atoms while the decrease at high energies is related to a drop in the cross section for defect production, as will be discussed below. The onset for defect production (minimum ion energy E_{min}) grows with ion mass via the kinematic factor (corresponding to a head-on collision) $E_{min} = T_d(m_C + M)^2 / (4m_C M)$, where T_d is the carbon atom displacement energy, and m_C and M are carbon atom and ion masses, respectively (for $M > m_C$). At higher energies, the impacts gave rise to morphological changes, i.e., formation of nonhexagonal rings while typically removing only one or two atoms from the target. The resulting structures remained sp^2 hybridized and flat. The extent of the changes can be estimated from the average defect size (total area of the hexagons transformed to other polygons), Fig. 1(e), combined with their probability to create a complex defect by a single irradiation event, Fig. 1(f). The peaks in probability for creating complex defects at lower energies for the two heaviest ions are mainly due to divacancies with accompanying small distortions, such as Frenkel pairs, created by the massive ions while penetrating through the membrane.

Although the typical defect size increases with ion energy, Fig. 1(e), this effect is compensated by decreasing probability for production of complex defects, Fig. 1(f). As the end

result, the average defect area decreases with increasing ion energy. For example, subjecting graphene to irradiation with Xe ions at the highest studied energy (2 MeV) will lead to a total defect area which is only approximately 30% of the total defect area after a similar dose with ion energies close to the SV and DV production maxima. A single defect at the highest energies spreads over about 60 \AA^2 but involves only approximately two removed atoms. This allows the lattice to reconstruct easily by saturating dangling bonds and forming a network of pentagons and heptagons with locally lowered density.²⁰

To understand the reason for the amorphization events at higher energies, we characterized the impact events by the energy ΔK lost by the ion while passing through graphene and the recoil angle of the closest carbon atom with respect to the normal of the graphene sheet ($\theta = 90^\circ$ corresponds to an in-plane direction). Obviously, for sufficient ΔK and $\theta \approx 0^\circ$, a single vacancy is always produced. At somewhat higher θ , DVs appear. At low ΔK , the DVs are created when the ion directly displaces two of the target atoms. At higher ΔK , DVs result from secondary recoils of the first displaced atom. When $\theta \rightarrow 90^\circ$, triple vacancies start to be formed, after which the large amorphization events dominate due to collision cascades within the graphene sheet. Although the exact ion energy for which the in-plane recoils become significant depends on the ion/carbon mass, the differences are minor in the energy range considered, as seen in Fig. 1(f).

Having analyzed the production of defects in an isolated graphene sheet by the AP MD method, we used the conventional BC approach as implemented in TRIM to assess the applicability of the method to simulations of irradiation effects in nanoscale systems. We assumed that the thickness of the graphene layers is 3.4 \AA and used graphite bulk density

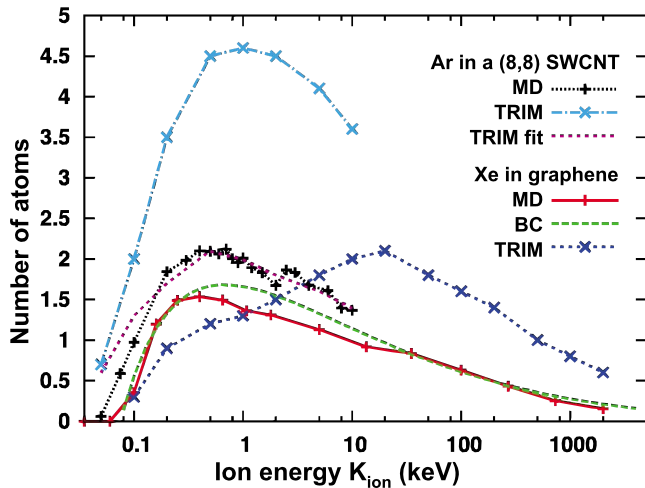


FIG. 2. (Color online) Average number of sputtered atoms as a function of ion energy as calculated by the analytical MD and semiempirical approach implemented in the code TRIM in graphene and a single-wall carbon nanotube. MD/BC values give the number of removed atoms, the TRIM value is the number of vacancies. The MD results for the SWCNT were calculated up to 10 keV (Ref. 14).

($\rho=2.25$ g/cm³). We did similar simulations for a (8,8) SWNT, the density ($\rho=1.57$ g/cm³) of which was computed under assumption that the nanotube diameter is the actual atomic diameter plus graphene layer thickness. In Fig. 2 we show the average number of displaced atoms from graphene and SWNT as a function of ion energy as calculated with AP MD and with the TRIM code.¹⁰ The position of the maximum on the curve for graphene obtained with TRIM differs by nearly two orders of magnitude from the more accurate MD results. The TRIM approach also gives considerably larger number of defects at high energies. Likewise, there is a substantial difference for the nanotube. Although we were able to fit the TRIM data to the MD results for the nanotube by choosing a nonrealistically low density, we were not able to do this for graphene.

In order to understand why the TRIM approach gives unreasonable results, we carried out additional calculations in which we mimicked the BC-based statistical approach. Now, the ion impact was modeled as a scattering event between the ion and a single carbon atom, and we assumed that a defect is produced if ΔK exceeds the T_d needed to produce a SV. For these calculations, we used $T_d=23$ eV, close to what is given by the DFT MD approach (see below). No further collisions were assumed. This setup leads to a binary scattering integral which can be evaluated numerically. As transferred energy increases with decreasing impact parameter p , there exists a maximum p which still leads to a displacement of the recoil atom. The probability of creating a vacancy can then be deduced taking into account the actual atomic density of graphene. The results of the BC calculations are also displayed in Fig. 2. It is evident that the fundamental problem in using the semiempirical approach implemented in TRIM for estimating ion irradiation damage in nanostructures is not the binary-collision approximation but the assumption of an amorphous target with a homogenous density. The dis-

crepancy between the BC and MD curves in Fig. 2 at the intermediate energies is due to the displacement events in which the ion simultaneously displaces more than one atom, where the BC approach is not valid. At higher energies the cross section decreases leading again to a binary collision, which will affect more than one target atom only via in-plane recoils.

To ensure that our AP method gives reasonable description of the irradiation process, we also carried out DFT MD simulations to evaluate the characteristic quantities from first principles. We used plane-wave basis set DFT code VASP (Ref. 21) with projector-augmented wave (PAW) potentials²² to describe the core electrons, and the generalized gradient approximation²³ for exchange and correlation. For simply displacing one carbon atom from pristine graphene, we obtained a $T_d=22.2 \pm 0.2$ eV and the minimum kinetic energy needed for an Ar atom to displace the C atom was $K_{ion}=32.74 \pm 0.15$ eV (a direct head-on collision perpendicular to the graphene layer). The corresponding values from the classical AP MD simulations were 22.05 eV and 32.33 eV, respectively, in a surprisingly good agreement with the first-principles results. As the reliability of the PAW method at small interatomic separations is not obvious *a priori*, we also compared the PAW calculations with all-electron calculations carried out with the simulation code DMOL (Ref. 24) for the C-Ar dimer and noticed that the PAW results are reasonable up to atom separations corresponding to ion energy of about 500 eV. Thus, the AP MD approach gives not only qualitatively but also quantitatively reasonable estimates of defect production during ion irradiation in carbon nanosystems.

As mentioned earlier, defects after high-energy impacts are quite rare, Fig. 1(f), but they extend to cover large areas around the impact points, Fig. 1(e), while only involving one or two missing atoms, Fig. 1(b). This result requires a method which takes into account the actual atomic structure, such as MD. Due to the ability of carbon nanostructures to reconstruct by forming nonhexagonal carbon rings,^{18,20,25} the final structure remains flat and sp^2 bonded with a somewhat lower density and/or few vacancies. However, this should not affect the gas-holding capacity, as recent simulations indicate.²⁶ Hence, one can use graphene as a membrane for ion-beam analysis on volatile targets or targets which should be kept under ambient conditions like works of art²⁷ or living cells.²⁸ Irradiation experiments on such systems are challenging due to the necessity to separate the target from the ion-beam system kept in vacuum. The membrane should be transparent to the ions while preventing the target and atmospheric molecules from entering the vacuum system. Because the total damaged area decreases with increasing ion energy, the use of graphene as a membrane is preferable at high energies. In Fig. 3 we compare the energy distribution of ions passing through graphene and those passing through a state-of-the-art 0.1 μm Si₃N₄ membrane²⁷ (with areal density approximately 170 times higher than that of graphene). It is clear that an ultimately narrow energy distribution for the ions passing through the membrane can be achieved by using graphene. As the number of sputtered atoms from the graphene sheet is low, using graphene also minimizes any effects produced by sputtered target atoms. In a similar manner, using graphene as a TEM transparent substrate²⁹ will

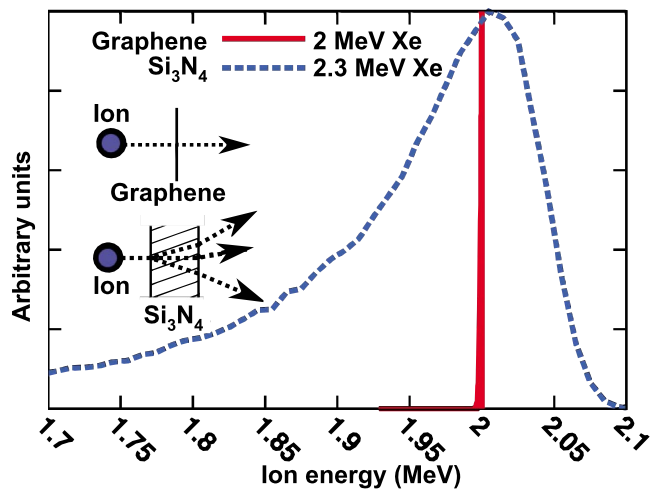


FIG. 3. (Color online) Energy profiles (distribution over energy) for Xe ions passing through a graphene layer (AP MD) and a $0.1 \mu\text{m}$ Si_3N_4 membrane (TRIM) with energies which lead to a peak at 2 MeV. Schematic presentations of both cases are presented in the inset. Note that the electronic stopping, neglected in the presented MD simulations, would shift the peak toward lower energies by less than 10 eV and introduce a minor deviation in the energies.

minimize backscattering in ion irradiation experiments on nanometer-sized objects.

To conclude, we used atomistic computer simulations based on analytical potential and density-functional theory models to study the production of defects in graphene under ion irradiation. We identified the types and concentrations of defects which appear in graphene under impacts of various ions with energies ranging from tens of electron volt to mega-electron volt and showed that all defects beyond single and double vacancies are formed via in-plane recoils, which is unique for two-dimensional materials. We further demonstrated by the examples of graphene and carbon nanotubes that the conventional approach developed for assessing the irradiation damage in bulk materials cannot be applied to low-dimensional systems, as it treats the target as amorphous medium without any account for the actual atomic structure. Finally, taking into account the gas-holding capacity of graphene, we suggest using graphene membranes for ion-beam analysis in volatile systems which cannot be put in high vacuum required for the operation of ion beams.

We thank the Finnish IT Center for Science for generous grants of computer time through the Grand Challenge program. This work was supported by the Academy of Finland through several projects and the Centre of Excellence program.

- ¹A. K. Geim and K. S. Novoselov, *Nature Mater.* **6**, 183 (2007).
- ²A. H. Castro Neto, F. Guinea, N. M. R. Peres, K. S. Novoselov, and A. K. Geim, *Rev. Mod. Phys.* **81**, 109 (2009).
- ³V. M. Pereira, F. Guinea, J. M. B. Lopes dos Santos, N. M. R. Peres, and A. H. Castro Neto, *Phys. Rev. Lett.* **96**, 036801 (2006).
- ⁴L. Tapasztó, G. Dobrik, P. Nemes-Incze, G. Vertesy, P. Lambin, and L. P. Biro, *Phys. Rev. B* **78**, 233407 (2008).
- ⁵J. H. Chen, W. G. Cullen, C. Jang, M. S. Fuhrer, and E. D. Williams, *Phys. Rev. Lett.* **102**, 236805 (2009).
- ⁶E. Stolyarova *et al.*, *Nano Lett.* **9**, 332 (2009).
- ⁷G. Compagnini *et al.*, *Carbon* **47**, 3201 (2009).
- ⁸M. Nastasi, J. Mayer, and J. Hirvonen, *Ion-Solid Interactions—Fundamentals and Applications* (Cambridge University Press, Cambridge, Great Britain, 1996).
- ⁹J. F. Ziegler, J. P. Biersack, and U. Littmark, *The Stopping and Range of Ions in Matter* (Pergamon, New York, 1985).
- ¹⁰J. F. Ziegler, *Nucl. Instrum. Methods Phys. Res. B* **219-220**, 1027 (2004).
- ¹¹A. V. Krasheninnikov and F. Banhart, *Nature Mater.* **6**, 723 (2007).
- ¹²J. S. Bunch *et al.*, *Nano Lett.* **8**, 2458 (2008).
- ¹³A. V. Krasheninnikov, Y. Miyamoto, and D. Tomanek, *Phys. Rev. Lett.* **99**, 016104 (2007).
- ¹⁴A. Tolvanen *et al.*, *Appl. Phys. Lett.* **91**, 173109 (2007).
- ¹⁵D. W. Brenner *et al.*, *J. Phys.: Condens. Matter* **14**, 783 (2002).
- ¹⁶H. J. C. Berendsen *et al.*, *J. Chem. Phys.* **81**, 3684 (1984).
- ¹⁷A. V. Krasheninnikov, *Solid State Commun.* **118**, 361 (2001).
- ¹⁸L. Sun *et al.*, *Science* **312**, 1199 (2006).
- ¹⁹A. J. Stone and D. J. Wales, *Chem. Phys. Lett.* **128**, 501 (1986).
- ²⁰R. G. Amorim *et al.*, *Nano Lett.* **7**, 2459 (2007).
- ²¹G. Kresse and J. Furthmüller, *Comput. Mater. Sci.* **6**, 15 (1996).
- ²²P. E. Blöchl, *Phys. Rev. B* **50**, 17953 (1994).
- ²³J. P. Perdew, K. Burke, and M. Ernzerhof, *Phys. Rev. Lett.* **77**, 3865 (1996).
- ²⁴B. Delley, *J. Chem. Phys.* **92**, 508 (1990).
- ²⁵J. Kotakoski, A. V. Krasheninnikov, and K. Nordlund, *Phys. Rev. B* **74**, 245420 (2006).
- ²⁶O. Leenaerts *et al.*, *Appl. Phys. Lett.* **93**, 193107 (2008).
- ²⁷J. Dran *et al.*, *Nucl. Instrum. Methods Phys. Res. B* **219-220**, 7 (2004).
- ²⁸V. Hable *et al.*, *Nucl. Instrum. Methods Phys. Res. B* **267**, 2090 (2009).
- ²⁹J. C. Meyer *et al.*, *Nano Lett.* **8**, 3582 (2008).